

# INFLUENCE OF THE TACHOCLINE ON SOLAR EVOLUTION

A. S. Brun<sup>1</sup> and J.-P. Zahn

*Département d'Astrophysique Stellaire et Galactique, Observatoire de Paris, Section Meudon, 92195 Meudon, France*

**Abstract.** Recently helioseismic observations have revealed the presence of a shear layer at the base of the convective zone related to the transition from differential rotation in the convection zone to almost uniform rotation in the radiative interior, the tachocline. At present, this layer extends only over a few percent of the solar radius and no definitive explanations have been given for this thinness. Following Spiegel and Zahn (1992, *Astron. Astrophys.*), who invoke anisotropic turbulence to stop the spread of the tachocline deeper in the radiative zone as the Sun evolves, we give some justifications for their hypothesis by taking into account recent results on rotating shear instability (Richard and Zahn, 1999, *Astron. Astrophys.*). We study the impact of the macroscopic motions present in this layer on the Sun's structure and evolution by introducing a macroscopic diffusivity  $D_T$  in updated solar models. We find that a time dependent treatment of the tachocline significantly improves the agreement between computed and observed surface chemical species, such as the  $^7\text{Li}$  and modify the internal structure of the Sun (Brun, Turck-Chièze and Zahn, 1999, *Astrophys. J.*).

to appear in the *Annals of the New York Academy of Sciences*, Vol 898.

## 1. INTRODUCTION

The presence of a shear layer connecting the differential rotation of the convective zone to the solid rotation of the radiative zone is now well established by helioseismic inversions (Figure 1 and [1]). Both its location and width are more and more constrained and seem to be  $0.691 \pm 0.004 R_\odot$  and less than  $0.05 R_\odot$ , respectively. Today, there are several hydrodynamical or MHD descriptions of this shear layer and its extension but none is definitive [2], [3], [4]. In these models the motions in the tachocline are either turbulent or laminar, involve magnetic field or are purely hydrodynamical. In this paper we discuss the basic ideas supporting the dynamical description of this transition layer. First, in Section 2 we recall the physical processes acting in this layer and summarize the different approaches with an emphasis on Spiegel and Zahn's description invoking a nonlinear anisotropic turbulence. In Section 3, using the prescription of

---

<sup>1</sup>Present address: JILA, University of Colorado, Boulder, CO 80309-0440, USA.

Spiegel and Zahn [2] for the amplitude of the vertical velocity in the tachocline and Chaboyer and Zahn [5] for the chemical mixing and evolution, we build solar models including a macroscopic diffusivity  $D_T$ , which are compared to the most recent helioseismic data and surface abundance observations for  ${}^7\text{Li}$ ,  ${}^9\text{Be}$  and  ${}^3\text{He}/{}^4\text{He}$  ratio. Finally, we summarize our results and conclude in Section 4.

## 2. THE SOLAR TACHOCLINE

The transition layer between the convective and radiative zones (Figure 1) plays a crucial role in our understanding of stars such as the Sun because it simultaneously involves several physical features, such as:

- the strong shear associated with the transition from differential to solid rotation, which may generate turbulence,
- a turbulent interface with the convection zone above, which may produce internal waves [6], [7],
- the possible presence of magnetic field, of fossile origin [3], or linked with the 11-year cycle [8],
- the proximity of the thermonuclear burning zone of lithium 7 and beryllium 9.

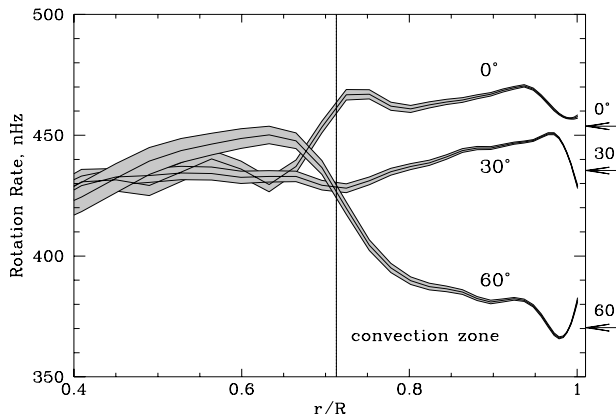


Figure 1. Solar rotation rate inferred from MDI data (aboard SOHO) as a function of radius at three latitudes,  $0^\circ$ ,  $30^\circ$  and  $60^\circ$  (the vertical line represents the base of the convection zone) [9].

In this section we shall concentrate on some specific points concerning the tachocline and we will not deal with the full complexity of this transition layer. The presence of a latitudinal differential rotation at the base of the convection zone induces a latitudinal temperature gradient  $\Omega(\theta) \rightarrow \nabla T(\theta)$ . Without any limiting process this temperature gradient will diffuse inwards, on a thermal diffusion time scale, enforcing differential rotation deep into the radiative interior of the Sun. As we already stated, however, helioseismic observations indicate a uniform rotation profile in the radiation zone, and thus we have to find which

processes could hinder this diffusion.

There are different possibilities and first and foremost is the stable stratification of the radiation zone. This effect would indeed slow down the spread of the tachocline, but in spite of that, the layer would still extend to one third of the radius in the present Sun, as estimated by Spiegel and Zahn [2], which is far too much. Thus another process must be invoked to explain the observed thinness of the tachocline.

One possibility is the presence of a magnetic field in the radiation zone, as advocated by Gough and McIntyre [3]. Their model is promising, but it has not yet been worked out in detail: it remains to be seen how the poloidal field threads into the convection zone, and avoids imposing differential rotation throughout the radiative interior.

Another possibility has been suggested by Spiegel and Zahn [2]. If the latitudinal shear is unstable, it could generate anisotropic turbulence which would tend to reduce the differential rotation, and hence prevent the spread of the tachocline. It is not clear whether the solar tachocline is linearly unstable: when one applies the criterion derived by Watson [10] to an angular velocity profile of the type  $\Omega \propto 1 - \alpha_1 \sin^2 \lambda$ , where  $\lambda$  is the latitude, linear instability requires  $\alpha_1 > 0.29$ , which is larger than the solar value  $\alpha_1 \approx 0.25$ . It appears, however, that a law of the type  $\Omega \propto 1 - \alpha_1 \sin^2 \lambda - \alpha_2 \sin^4 \lambda$ , closer to the latitudinal dependence drawn from helioseismic inversions (see Fig. 1) would be more sensitive to such instability [11]. Furthermore, a toroidal magnetic field of sufficient strength would also act to destabilize the flow, as shown by Gilman and Fox [4]. In any case, the Reynolds number is so high that such a differential rotation would be liable to finite amplitude instability, as can be inferred from laboratory experiments [12]. It has been argued by Gough and McIntyre [3] that turbulence does not necessarily reduce the shear of differential rotation: in the Earth's atmosphere the transport of angular momentum would even imply a negative viscosity. But there the transport is achieved mainly through Rossby waves, and it is not clear whether this can be applied to the solar tachocline.

Admittedly, this important issue is still a matter of debate, and it may be settled only by comparing the models' predictions with the observed properties of the Sun. This is why we have chosen to draw all observable consequences from the model which has been worked out in sufficient detail to allow such a test, namely the turbulent tachocline proposed by Spiegel and Zahn [2]. We will show that the mixing induced in this model improves both the sound speed profile (reduction of the peak below the convection zone) and the surface light element abundances, confirming the need of introducing macroscopic processes in solar models [13]-[15].

### 3. MIXING IN THE SOLAR TACHOCLINE: PHYSICAL DESCRIPTION

Macroscopic mixing may be treated in solar models by adding an effective diffusivity  $D_T$  in the equation for the time evolution of the concentration of chemical species. To establish this coefficient for the tachocline, we use the description by Spiegel and Zahn [2], where anisotropic turbulence is responsible for stopping the spread of the layer. This anisotropic diffusion will also interfere with the

advective transport of chemicals. Chaboyer and Zahn [5] have shown that the result is a diffusive transport in the vertical direction. Using their result, Brun, Turck-Chièze and Zahn [16] derived the following expression for the macroscopic diffusivity:

$$D_T(r) = \frac{4}{405} \nu_H \left( \frac{d}{r_{bcz}} \right)^2 \mu_4^6 Q_4^2 \exp(-2\zeta) \cos^2(\zeta) + \text{higher order terms} \quad (1)$$

with  $Q_4 = \tilde{\Omega}_4/\Omega$ ,  $\tilde{\Omega}_4$  characterizing the differential rotation rate,  $\mu_4 = 4.933$ ,  $\zeta = \mu_4(r_{bcz} - r)/d$  a non-dimensional depth,

$$d = r_{bcz}(2\Omega/N)^{1/2}(4K/\nu_H)^{1/4} \quad (2)$$

a length related to the tachocline thickness  $h$  (e.g  $h \sim d/2$ ),  $r_{bcz}$  the radius,  $\Omega$  the angular velocity and  $K = \chi/\rho c_p$  the radiative diffusivity at the base of the convective zone. The horizontal component of the macroscopic diffusivity  $D_H$  is assumed to be equal to the horizontal viscosity  $\nu_H$ . In our solar models, we treat  $h$  (hence  $d$ ) as an adjustable parameter, chosen to agree with the helioseismic determination of the tachocline thickness  $h \leq 0.05R_\odot$  [1]. With the latitudinal dependence of the angular velocity at the base of the convection zone deduced from Thompson et al. [17],  $\Omega_{bcz}/2\pi = 456 - 72x^2 - 42x^4$  nHz (with  $x = \sin \lambda$ ), we have reestimated the coefficient  $Q_4 = -1.707 \times 10^{-2}$ , as well as the ratio between the rotation in the deep radiative zone and the equatorial rate  $\Omega/\Omega_0 = 0.9104$ . The prediction by Gough and Sekii [18] for the latter, who consider instead the magnetic stresses, is  $\sim 0.96$ ; presently, the seismic observations suggest a rotational ratio of  $0.94 \pm 0.01$  [1], which is intermediate between these two theoretical estimates.

An analysis of the dependence of our  $d$  and  $D_T$  with the global and differential rotation rates yields

$$D_T \propto \nu_H \left( \frac{d}{r_{bcz}} \right)^2 Q_i^2 \propto \Omega \nu_H^{1/2} (\hat{\Omega}/\Omega)^2, \quad d \propto \Omega^{1/2} / \nu_H^{1/4}. \quad (3)$$

where we have used equations (1) and (2). Assuming that the turbulent viscosity is proportional to the differential rotation (i.e.,  $\nu_H \propto \hat{\Omega}$ ), as suggested by the laboratory experiments [12], and introducing the dependence of the differential rotation on rotation observed by Donahue, Saar and Baliunas [19] ( $\hat{\Omega} \propto \Omega^{0.7 \pm 0.1}$ ), we finally obtain the following scalings

$$D_T \propto \Omega^{0.75 \pm 0.25}, \quad d \propto \Omega^{(1.3 \mp 0.1)/4}. \quad (4)$$

We conclude that the tachocline mixing was stronger in the past both because that layer was thicker and because the diffusivity was larger. We render the mixing in the tachocline time dependent, through  $D_T(\Omega(t))$  and  $d(\Omega(t))$ , by using the spin-down law  $\Omega \propto t^{-1/2}$  which was deduced by Skumanich [20] from the rotation rate of stellar clusters of different ages.

## 4. RESULTS

Starting from the reference model of Brun, Turck-Chièze and Morel [21] built with the CESAM code [22], we introduce for this study the nuclear reaction  ${}^7\text{Li}(p,\alpha){}^4\text{He}$  proposed by Engstler et al. [23] and the coefficient  $D_T$  (Eq. 1) in the diffusion equation of chemical species, and we follow the time evolution of the solar model from the pre-main sequence (PMS) until 4.6 Gyr. The results are shown in the Table 1 and Figures 2-5 (see Ref. [15] for a more detailed discussion). We use a tachocline thickness  $h$  of 0.05 or 0.025  $R_\odot$ ,  $N$  of 100 or 25  $\mu\text{Hz}$  and  $\Omega$  of 0.415  $\mu\text{Hz}$ . Our standard model [21] has a surface abundance for helium of 0.2427 in mass, corresponding to an  ${}^4\text{He}$  diffusion of 10.8%. This value of  $Y_s$  is a bit too low if we compare with the Basu and Antia [24] value for the OPAL equation of state [25],  $Y_s = 0.249 \pm 0.003$ .

Table 1. Surface abundance variation of  ${}^3\text{He}/{}^4\text{He}$  during the last 3 Gyr, surface abundances of  ${}^4\text{He}$  and heavy elements  $Z$ , and abundance ratio initial/surface for  ${}^7\text{Li}$  and  ${}^9\text{Be}$  from observations and for solar models at the solar age<sup>a</sup>

	Obs	Ref	$A$	$B$	$A_t$	$B_t$	$B_{tz}$	$C_t$
$d(r/R_\odot)$	$\leq 0.1$	-	0.1	0.1	0.1	0.1	0.1	0.05
$N$ ( $\mu\text{Hz}$ )	-	-	100	25	100	25	25	25
$({}^3\text{He}/{}^4\text{He})_s$	max 10%	2.28%	2.14%	2.01%	2.11%	2.0%	2.02%	2.07%
${}^4\text{He}_s$	$0.249 \pm 0.003$	0.2427	0.2452	0.2473	0.2455	0.2477	0.2509	0.2464
$(Z/X)_s$	$0.0245 \pm 0.002$	0.0245	0.0245	0.0245	0.0245	0.0245	0.0255	0.0245
${}^7\text{Li}_0/{}^7\text{Li}_s$	$\sim 100$	$\sim 6$	$\sim 8$	$\sim 22$	$\sim 12$	$\sim 91$	$\sim 134$	$\sim 89$
${}^9\text{Be}_0/{}^9\text{Be}_s$	$1.10 \pm 0.03$	1.115	1.093	1.086	1.093	1.118	1.125	1.092

<sup>a</sup>Subscripts  $t$  for time dependent models,  $tz$  for time dependent model with  $Z_0 = Z_0^{ref} = 0.01959$

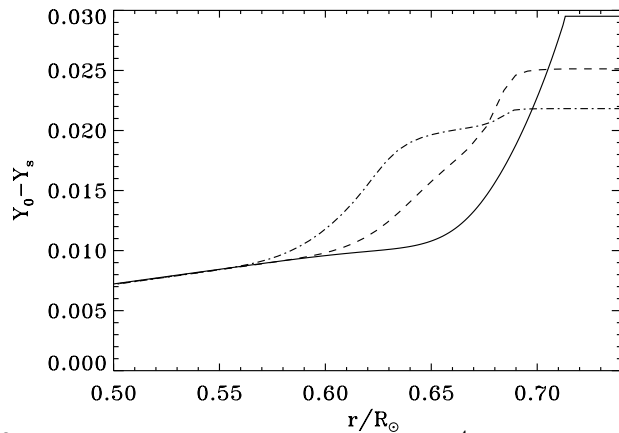


Figure 2. Radial profile of the difference of  ${}^4\text{He}$  composition between the initial and present values for the reference solar model including only microscopic diffusion (*solid line*) and solar models where we add a macroscopic mixing due to the presence of the tachocline: coefficient  $A$  (*dash*) and  $B$  (*dash dot*) (see Table 1 for the model characteristics).

When introducing our diffusive coefficient, we mix helium back into the convection zone, inhibiting the microscopic diffusion up to 25% and producing a photospheric  ${}^4\text{He}_s = 0.2473$  (cf. Table 1, models  $A$  and  $B$ ). As expected,

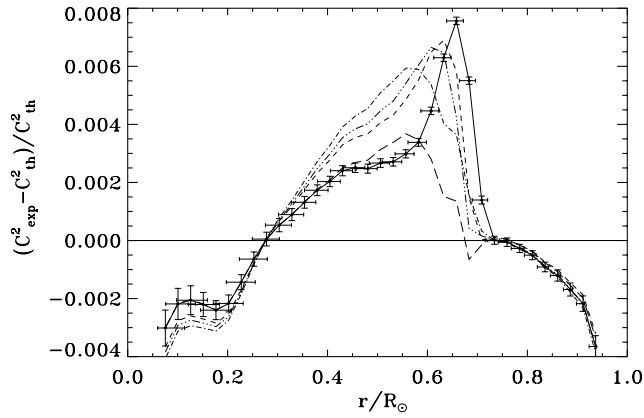


Figure 3. Squared sound speed difference between GOLF+MDI data and the reference model (*solid line*) or models including a turbulent term: coef  $A_t$  ( $d = 0.1$ ,  $N = 100$ ) (*dash*),  $B_t$  ( $d = 0.1$ ,  $N = 25$ ) (*dash dot*),  $C_t$  ( $d = 0.05$ ,  $N = 25$ ) (*dash three dots*), and one model with  $B_t$  and  $Z_0 = Z_0^{ref} = 0.01959$  (i.e.,  $B_{tz}$ ) (*long dash*).

the composition profile is smoother and flattens over the distance  $h$  below the convective zone (see Figure 2).

The effect on the sound speed is displayed in Figure 3. When the macroscopic transport is neglected, the squared sound speed difference reveals a peak just below the convection zone, coinciding with the tachocline (*solid line*). Macroscopic diffusion acts to reduce this peak, but when one recalibrates the model to yield, e.g., the present abundance of heavy elements ( $Z/X = 0.0245 \pm 0.002$ ), the effect is rather minor. On the other hand, if the heavy elements are let free to adjust, within the observational uncertainties, the peak is completely removed, leaving only a broad bump culminating at  $0.6 R_\odot$ , which presumably is due to another cause (*long dashed line*).

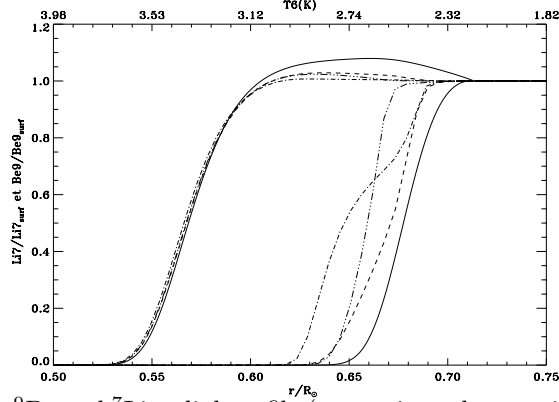


Figure 4.  $^9\text{Be}$  and  $^7\text{Li}$  radial profile (approximately superimposed the temperature scale) for several models: respectively, reference (*solid line*), coefficient  $A_t$  (*dash*), coefficient  $B_t$  (*dash dot*) and coefficient  $C_t$  (*dash three dots*).

The two light elements  $^7\text{Li}$  and  $^9\text{Be}$  are extremely sensitive to mixing processes occurring in stars because their nuclear burning temperatures are rather low (respectively,  $2.5 \cdot 10^6$ , and  $3.2 \cdot 10^6$  K) [26]. The new observational constraints

can only be satisfied if those chemical species are mixed in a rather thin layer below the convective zone, in order to preserve  ${}^9\text{Be}$ , which is very little depleted according to Balachandran and Bell [27]. This is the case with our tachocline model. However, if the mixing had proceeded in the past at the same rate as in the present Sun,  ${}^7\text{Li}$  would have been depleted only by a factor  $\sim 4$ , which is insufficient to account for the photospheric lithium abundance ([28] and references therein). But the thickness of the tachocline and the strength of mixing have been larger in the past, when the Sun was rotating faster. This effect is included in the models labeled with the index  $t$  (as  $B_t$ ), whose evolution was calculated with the time-dependent diffusivity of Eq. (4).

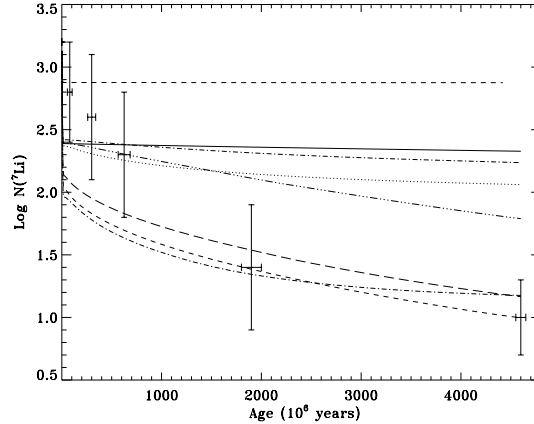


Figure 5. Time dependent depletion of  ${}^7\text{Li}$  for several solar models: no microscopic diffusion (*dash*), with microscopic diffusion (*solid line*) and with mixing in the tachocline thickness: coefficient  $A$  (*dash dot*),  $B$  (*dash three dots*), then with time dependent mixing  $A_t$  (*dots*),  $B_t$  (*long dash*),  $C_t$  (*thick dash dot*) and  $B_{tz}$  ( $Z_0 = Z_0^{ref} = 0.01959$ ) (*thick dash*). We superimposed on the theoretical curves the open cluster observations (adapted from Vauclair and Richard [14] and cluster age uncertainties deduced from Lebreton et al. [29]).

In Table 1 we give the initial over present ratio of  ${}^7\text{Li}$  and  ${}^9\text{Be}$  and show in Figure 4 the radial profile of  ${}^7\text{Li}$  and  ${}^9\text{Be}$  normalized to the surface abundance. We clearly see that the mixing process modifies the distribution of lithium but not that of beryllium (exception being the flat plateau for the mixed models in comparison with the “pure” diffusive one). With the coefficients  $B$  more  ${}^7\text{Li}$  is burned than with  $A$ , and we also see that the time dependence (models with index  $t$ ) improves the  ${}^4\text{He}$  surface abundance as well as the  ${}^7\text{Li}$  depletion, where a value of  $\sim 100$  is obtained without destroying  ${}^9\text{Be}$  or increasing too much the  ${}^3\text{He}/{}^4\text{He}$  surface ratio over the past 3 Gyr, as deduced by Geiss and Gloeckler [30] from meteorites and solar wind abundance measurements (see Table 1).

In Figure 5 we show the lithium depletion occurring during the Sun’s evolution for the different models presented, plus a model without any diffusion. Clearly, only the diffusive models including mixing in the tachocline yield a substantial depletion during main sequence evolution, in agreement with the observations (superimposed with their inherent dispersion on the theoretical curves). Note that the strong time dependent mixing with  $N = 25$  (models  $B_t$ ,  $C_t$  and  $B_{tz}$ ) presents a reasonable value of the solar  ${}^7\text{Li}$  depletion ( $\sim 100$ ).

However the lithium depletion during the PMS is probably overestimated due to the crude spin-down law we have adopted. A more detailed analysis of these phases is under study, including metallicity effects and more appropriate angular momentum evolution during this phase.

Our results show the interest to follow together the photospheric abundance of the four elements  $^3\text{He}$ ,  $^4\text{He}$ ,  $^7\text{Li}$ ,  $^9\text{Be}$ , and to examine their sensitivity to the microscopic, as well as the macroscopic, processes. This study encourages the introduction of macroscopic processes in stellar evolution models, and demonstrates the crucial role of the thin tachocline layer below the convective zone.

## References

1. Corbard, T., L. Blanc-Féraud, G. Berthomieu & J. Provost. 1999. Non linear regularization for helioseismic inversions. Application for the study of the solar tachocline. *Astron. Astrophys.* **344**: 696-708.
2. Spiegel, E. A. & J.-P. Zahn. 1992. The solar tachocline. *Astron. Astrophys.* **265**: 106-114.
3. Gough, D.O. & M.E. McIntyre. 1998. Inevitability of a magnetic field in the Sun's radiative interior. *Nature*. **394**: 755-757.
4. Gilman, P.A. & P.A. Fox. 1997. Joint instability of latitudinal differential rotation and toroidal magnetic fields below the solar convection zone. *Astrophys. J.* **484**: 439-454.
5. Chaboyer, B. & J.-P. Zahn. 1992. Effect of horizontal turbulent diffusion on transport by meridional circulation. *Astron. Astrophys.* **253**: 173-177.
6. Press, W.H. 1981. Radiative and other effects from internal waves in solar and stellar interiors. *Astrophys. J.* **245**: 286-303.
7. Schatzman, E. 1993. Transport of angular momentum and diffusion by the action of internal waves. *Astron. Astrophys.* **279**: 431-446.
8. Choudhuri, A.M., M. Schüssler & M. Dikpati. 1997. The solar dynamo with meridional circulation. **319**: 362-362.
9. Kosovishev et al. 1997. Structure and rotation of the solar interior: Initial results from the MDI medium-l program. *Sol. Phys.* **170**: 43-61.
10. Watson, M. 1981. Shear instability of differential rotation in stars. *Geophys. Astrophys. Fluid Dynam.* **16**: 285-298.
11. Garaud, P. & D.O. Gough. 1999 (private communication)
12. Richard, D. & J.-P. Zahn. 1999. Turbulence in differentially rotating flows. What can be learned from the Couette-Taylor experiment. *Astron. Astrophys.* **347**: 734-738.
13. Zahn, J.-P. 1998. Macroscopic transport. Large-scale advection, turbulent diffusion, wave transport. *Space Sc. Rev.* **85**: 79-90.
14. Vauclair, S. & O. Richard. 1998. Consistent solar models including the  $^7\text{Li}$  and  $^3\text{He}$  constraints. in *Structure and Dynamics of the Interior of the Sun and Sun-like Stars*, S. G. Korzennik & A. Wilson Eds. ESA SP-418, Vol 1: 427-429. ESA Publication Division, Noordwijk, The Netherlands.



15. Brun, A.S., S. Turck-Chièze & J.-P. Zahn. 1999. Standard solar models in the light of new helioseismic constraints. II. Mixing below the convective zone. *Astrophys. J.* **525**: 1032-1041.
16. Brun, A.S., S. Turck-Chièze & J.-P. Zahn. 1998. Macroscopic processes in the solar interior. in *Structure and Dynamics of the Interior of the Sun and Sun-like Stars*. S. G. Korzennik & A. Wilson Eds. ESA SP-418, Vol 1: 439-443. ESA Publication Division, Noordwijk, The Netherlands.
17. Thompson, M.J., J. Toomre and the GONG Dynamics Inversion Team 1996. Differential rotation and dynamics of the solar interior. *Science*. **272**: 1300-1305.
18. Gough, D.O. & T. Sekii. 1997. On the solar tachocline. in *IAU 181 Sounding Solar and Stellar Interior* (poster volume). J. Provost & F. X. Schmider Eds: 93-94. Observatoire de la Côte d'Azur. Nice. France.
19. Donahue, R.A., S.H. Saar & S.L. Baliunas. 1996. A relationship between mean rotation period in lower main-sequence stars and its observed range. *Astrophys. J.* **466**: 384-391.
20. Skumanich, A. 1972. Time scales for CA II emission decay, rotational braking, and lithium depletion. *Astrophys. J.* **171**: 565-567.
21. Brun, A.S., S. Turck-Chièze & P. Morel. 1998. Standard solar models in the light of new helioseismic constraints. I. The solar core. *Astrophys. J.* **506**: 913-925.
22. Morel, P. 1997. CESAM: A code for stellar evolution calculations. *Astron. Astrophys. Sup.* **124**: 597-614.
23. Engstler et al. 1992. Test for isotopic dependence of electron screening in fusion reactions. *Phys. Lett. B.* **279**: 20-24.
24. Basu, S. & H.M. Antia. 1995. Helium abundance in the solar envelope. *Mon. Not. Roy. Astron. Soc.* **276**: 1402-1408.
25. Rogers, F.J., J. Swenson & C. Iglesias. 1996. OPAL equation-of-state tables for astrophysical Applications. *Astrophys. J.* **456**: 902-908.
26. Baglin, A. & Y. Lebreton. 1990. Surface abundances of light elements as diagnostic of transport processes in the Sun and solar-type stars. in *Inside the Sun*. G. Berthomieu & M. Cribier Eds. *Astrophysics and Space Science Library* 159: 437-448. Kluwer Academic Publishers. Netherlands.
27. Balachandran, S. & R.A. Bell. 1998. Shallow mixing in the solar photosphere inferred from revised beryllium abundances. *Nature*. **392**: 791-793.
28. Cayrel, R. 1998. Lithium abundances in low-z stars. *Space Sc. Rev.* **84**: 145-154.
29. Lebreton Y., A.E. Gomez, J.-C. Mermilliod, M.A.C. Perryman. 1997. The age and helium content of the Hyades revisited. in *Proceedings of the ESA Symposium 'Hipparcos- Venice '97'*. ESA SP-402: 231-236. ESA Publication Division, Noordwijk, The Netherlands.
30. Geiss, J. & G. Gloeckler. 1998. Abundances of deuterium and helium-3 in the protosolar cloud. *Space Sc. Rev.* **84**: 239-250.